Biosensors and Bioelectronics 30 (2011) 315–319

Contents lists available at SciVerse ScienceDirect

Biosensors and Bioelectronics

journal homepage: www.elsevier.com/locate/bios

Short communication

Au-nanoclusters incorporated 3-amino-5-mercapto-1,2,4-triazole film modified electrode for the simultaneous determination of ascorbic acid, dopamine, uric acid and nitrite

Cun Wang, Ruo Yuan*, Yaqin Chai, Yu Zhang, Fangxin Hu, Meihe Zhang

Key Laboratory of Analytical Chemistry (Chongqing), College of Chemistry and Chemical Engineering, Southwest University, Chongqing 400715, PR China

ARTICLE INFO

Article history:
Received 6 June 2011
Received in revised form 11 August 2011
Accepted 25 August 2011
Available online 16 September 2011

Keywords:
3-Amino-5-mercapto-1,2,4-triazole
Au-nanoclusters
Dopamine
Ascorbic acid
Uric acid
Nitrite

ABSTRACT

A novel biosensor has been constructed by the electrodeposition of Au-nanoclusters (nano-Au) on poly(3-amino-5-mercapto-1,2,4-triazole) (*p*-TA) film modified glassy carbon electrode (GCE) and employed for the simultaneous determination of dopamine (DA), ascorbic acid (AA), uric acid (UA) and nitrite (NO_2^-). NH_2 and SH groups exposed to the *p*-TA layer are helpful for the electrodeposition of nano-Au. The combination of nano-Au and *p*-TA endow the biosensor with large surface area, good biological compatibility, electricity and stability, high selectivity and sensitivity and flexible and controllable electrodeposition process. In the fourfold co-existence system, the linear calibration plots for AA, DA, UA and NO_2^- were obtained over the range of 2.1–50.1 μM, 0.6–340.0 μM, 1.6–110.0 μM and 15.9–277.0 μM with detection limits of 1.1×10^{-6} M, 5.0×10^{-8} M, 8.0×10^{-8} M and 8.9×10^{-7} M, respectively. In addition, the modified biosensor was applied to the determination of AA, DA, UA and NO_2^- in urine and serum samples by using standard adding method with satisfactory results.

© 2011 Elsevier B.V. All rights reserved.

1. Introduction

Dopamine (DA) is an important catecholamine neurotransmitter compound that has been paid much attention in the recent years. It plays a very important role in the functioning of central nervous, hormonal and cardiovascular systems (Li and Lin, 2006; Lin et al., 2007a). Abnormal levels of DA will lead to neurological disorders such as Parkinson's disease, senile dementia, schizophrenia and to HIV infection (Huang et al., 2008; Lin et al., 2007b). Uric acid (UA) is another important biomolecule present in urine and blood. Several diseases, such as gout, hyperuricaemia, and Lesch–Nyhan syndrome, will appear when the levels of UA are extreme abnormalities (Kalimuthu and John, 2009a; Liu et al., 2011). Ascorbic acid (AA) is a vital component in human diet and the animal and plant kingdoms. Moreover, AA is widely used for the prevention of scurvy and treatment of common cold, mental illness, cancer and AIDS (Kalimuthu and John, 2010; Li and Lin, 2006). Some groups have reported that NO can enhance or inhibit the release of DA (Guevara-Guzmam et al., 1994; Zhang et al., 2011). As known to all, in the central nervous system, NO can be oxidized to NO_2^- as fast as in a few seconds in biological circumstance. From the information above, we can conclude that NO_2^-, UA, DA and AA usually coexist in real biological samples. Therefore, the development of a sensitive and selective biosensor for their simultaneous determination is highly desirable for analytical applications and diagnostic researches. However, it is very difficult to determine the four species directly not only because the oxidation potentials of these species are too close to be separately, but also the electrode fouling which takes place due to the adsorption of oxidation products leads to poor selectivity (Atta et al., 2010; Lin et al., 2007b). Besides, many reported detection methods are complicated, expensive, and suffered from sensitivity as well as reproducibility. To overcome these problems, various materials have been utilized to construct biosensors, such as single-walled carbon nanohorn (Zhu et al., 2009), polymers (Zhang et al., 2009), nanoparticles (Atta et al., 2010) and boron-doped carbon nanotubes (Deng et al., 2009).

In recent years, the methods of formation of the polymer film and deposition of metal nanoparticles have attracted tremendous attention in electroanalysis because of the probable electronic interactions between the nanoparticles and groups in the polymer (Gopalan et al., 2007). Among the different methods for preparing polymers modified electrode, electropolymerization is a good choice to immobilize the polymer. Furthermore, the film thickness and permeation characteristics can be controlled. Also, the modified electrodes prepared by electropolymerization have obvious advantages in the detection of analytes. For example, it has high stability, selectivity and sensitivity due to the film homogeneity

* Corresponding author at: College of chemistry and chemical engineering, southwest university, Chongqing Key Laboratory of Analytical Chemistry, Chongqing, 400715, PR China. Tel.: +86 23 68252277; fax: +86 23 68253172.
E-mail address: yuanruo@swu.edu.cn (R. Yuan).

0956-5663/$ – see front matter © 2011 Elsevier B.V. All rights reserved.
doi:10.1016/j.bios.2011.08.035

in electrochemical deposition, strong adherence to the electrode surface and large surface area (Lin et al., 2007b; Zhang et al., 2009). Noble nanoparticles can provide a more similarly native environment than other metal nanoparticles because of its high catalytic activity, useful biocompatible ability (Li and Lin, 2006; Thiagarajan and Chen, 2007). It has been demonstrated that the noble nanoparticles modified electrodes showed excellent selectivity and sensitivity response towards several biomolecules. For example, palladium/poly (3,4-ethylenedioxythiophene) (Harish et al., 2008), gold nanoparticles/choline (Wang et al., 2007) and Pd-nanoclusters/poly(N-methylpyrrole) (Atta et al., 2010) modified electrodes have been used for the determination of AA, DA or UA. However, to the best of our knowledge, no articles have been reported for the simultaneous determination of AA, DA, UA and NO_2^- with easy fabrication, acceptable stability and good reproducibility as well as high sensitivity. Therefore, the development of a novel biosensor for sensitive simultaneous determination of the four substances is desirable.

3-Amino-5-mercapto-1,2,4-triazole (TA) is a low molecular weight chemical which has five potential coordination sites: three N cyclic atoms, one exocyclic NH_2 group and one exocyclic SH group (Baraldi et al., 1996; Sun et al., 2006). The *p*-TA modified layer containing numerous groups such as NH_2 and SH, which could facilitate the modification of Au-nanoclusters (nano-Au). Considering above, a novel biosensor was constructed by electropolymerizing TA film incorporated with nano-Au and used for the simultaneous determination of AA, DA, UA and NO_2^- at low levels. It was found that the nano-Au/*p*-TA modified biosensor exhibited high electrocatalytic activities towards the oxidation of AA, DA, UA and NO_2^-. In a word, the integration of nano-Au and *p*-TA can offer potential promise for the fabrication of biosensor.

2. Materials and methods

2.1. Reagents and chemicals

Uric acid (UA) and 3-amino-5-mercapto-1,2,4-triazole (TA) were purchased from Sigma Chemical Co. (St. Louis, MO, USA). Gold chloride ($HAuCl_4$) was obtained from Shanghai Chemical Reagent Co. (Shanghai, China). Sodium nitrite ($NaNO_2$), ascorbic acid (AA) and dopamine (DA) were purchased from Chemical Reagent Co. (Chongqing, China). Phosphate buffer solutions (PBS) (0.1 M) at various pH were prepared using 0.1 M Na_2HPO_4, 0.1 M KH_2PO_4, and 0.1 M KCl. Twice-distilled water was used throughout the experiments.

2.2. Apparatus

Differential pulse voltammetry measurements and cyclic voltammetric measurements experiments were performed with a CHI 660D electrochemical work station (Shanghai Chenhua Instrument Co., China). The conventional three-electrode system included a modified electrode as working electrode, a saturated calomel reference electrode (SCE), and a platinum wire auxiliary electrode. The morphological characterization of films was examined by scanning electron microscope (SEM, S-4800, Hitachi, Japan). Atomic force microscopy (AFM) images were taken using scanning probe microscope (Vecco, USA). All measurements were taken out at an appropriate potential and carried out on a static cell after uniform mixing at room temperature.

2.3. Preparation of nano-Au/p-TA modified electrode

Glassy carbon electrode (GCE, diameter 4.0 mm) was respectively polished with 0.3 and 0.05 μm alumina slurry, and then rinsed ultrasonically with ethanol and water for several minutes, successively.

Electropolymerization of TA on the GCE was carried out by 15 successive potential sweeps between −0.2 and 1.7 V at 0.05 V/s in 1 mM of TA containing 0.1 M H_2SO_4 (Kalimuthu and John, 2009b). Throughout the studies we have used 15 cycles deposited TA film because it showed the highest sensitivity towards the biomolecules (Fig. 1S). The *p*-TA modified electrode was denoted as *p*-TA/GCE. Subsequently, the *p*-TA/GCE was washed with doubly distilled water, and then scanned by CVs in 0.1 M PBS (pH 4.0) so as to gain a steady polymer film. The deposition of nano-Au on the *p*-TA/GCE was carried out according to the literature (Wang et al., 2007). Then the *p*-TA/GCE was performed by applying −0.2 V for 80 s in a mixture of H_2SO_4 (0.5 M) and $HAuCl_4$ (1 mM). The 80 s was the optimal deposition time according to our studies (Fig. 2S). The obtained electrode was described as nano-Au/*p*-TA/GCE.

For the sake of comparison, *p*-TA/GCE and nano-Au/GCE were also prepared under the same conditions.

3. Results and discussion

3.1. The characterization of the modified electrode

The surface topographies of different modified films were analyzed by scanning electron microscopy (SEM) and atomic force microscopy (AFM), respectively. Fig. 1A and B depictured the SEM micrographs of *p*-TA and nano-Au/*p*-TA films, respectively. As shown in Fig. 1A, the *p*-TA film appears a homogeneous surface. However, after electrodeposition of nano-Au (Fig. 1B), the SEM image of nano-Au/*p*-TA film clearly shows the presence of numerous, well distributed gold nanoparticles, suggesting nano-Au has been electrodeposited onto the *p*-TA film. Fig. 1C and D displayed the AFM micrographs of *p*-TA and nano-Au/*p*-TA films, respectively. As Fig. 1A, the AFM image of *p*-TA film (Fig. 1C) further presents a homogeneous surface. Furthermore, irregularly continuous small wrinkles were observed. Also, Fig. 1D gave similar results as Fig. 1B. The nano-Au was assembled to form an egg-shaped or hill-like nanostructures structure, and they were homogeneously distributed with average diameter of approximately 300 nm forming three-dimensional film structure. This result indicates the successful assembly of *p*-TA and nano-Au/*p*-TA film on the electrode surface.

3.2. Cyclic voltammetric behaviors of the modified electrode

The cyclic voltammograms (CVs) of different modified electrodes in 0.1 M PBS (pH 4.0) were investigated. As can be seen from Fig. 2A, *p*-TA/GCE (curve b) shows an apparently larger background current than the bare GCE (curve a), indicating that the film of *p*-TA firmly polymerized on the electrode surface. After modified with nano-Au, the background signal increased for nano-Au/*p*-TA/GCE (curve c) and this was attributed to the high specific area of nano-Au. The inset of Fig. 2A shows the electropolymerization process of GCE. Here, the anodic and cathodic peak potentials tended to be stable towards 15 scans. This observation may imply a self-adjustment of the polymer film thickness at the GCE (Ensafi and Khayamian, 2009).

In order to demonstrate the performance of nano-Au/*p*-TA/GCE, we compared the CV responses on different modified electrodes in 0.1 M PBS (pH 4.0) containing 160 μM AA, 10 μM DA, 20 μM UA and 60 μM NO_2^-. Fig. 2B shows that the bare GCE (curve a) and nano-Au/GCE (curve c) only gave a broad anodic peak for DA, AA and UA, and an inconspicuous anodic peak for NO_2^-. For *p*-TA/GCE (curve b), the peak currents of DA and UA were notably improved and the selectivity was better than that at the bare GCE and nano-Au/GCE, but simultaneous determination of AA, DA, UA and NO_2^- could not be obtained due to the indistinguishable and small response to NO_2^- and AA. In contrast, four well-defined voltammetric peaks

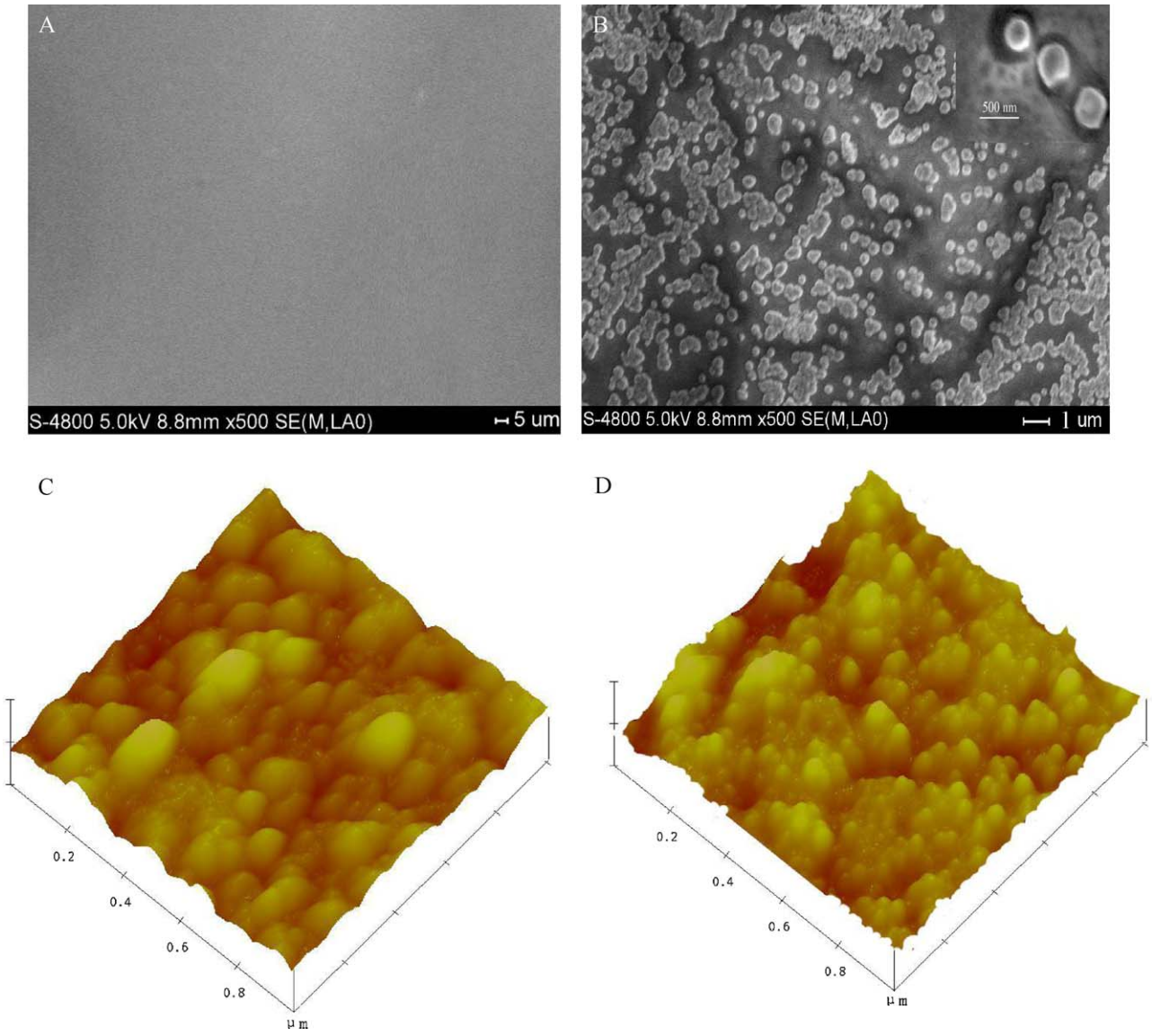

Fig. 1. SEM images of (A) *p*-TA/GCE and (B) nano-Au/*p*-TA/GCE and AFM images of (C) *p*-TA/GCE and (D) nano-Au/*p*-TA/GCE.

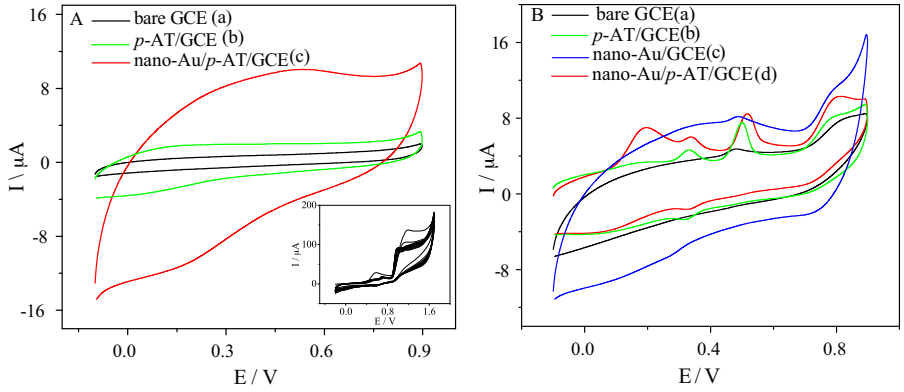

Fig. 2. (A) CV responses of (a) bare GCE, (b) *p*-TA/GCE and (c) nano-Au/*p*-TA/GCE in 0.1 M PBS (pH 4.0). Inset of part (A) shows the electropolymerization process of GCE in 1 mM of TA containing 0.1 M H_2SO_4 in the range of −0.2 and 1.7 V for 15 cycles at 0.05 V/s. (B) CVs at (a) bare GCE, (b) *p*-TA/GCE, (c) nano-Au/GCE and (d) nano-Au/*p*-TA/GCE in 0.1 M PBS (pH 4.0) containing containing 160 μM AA, 10 μM DA, 20 μM UA and 60 μM NO_2^-.

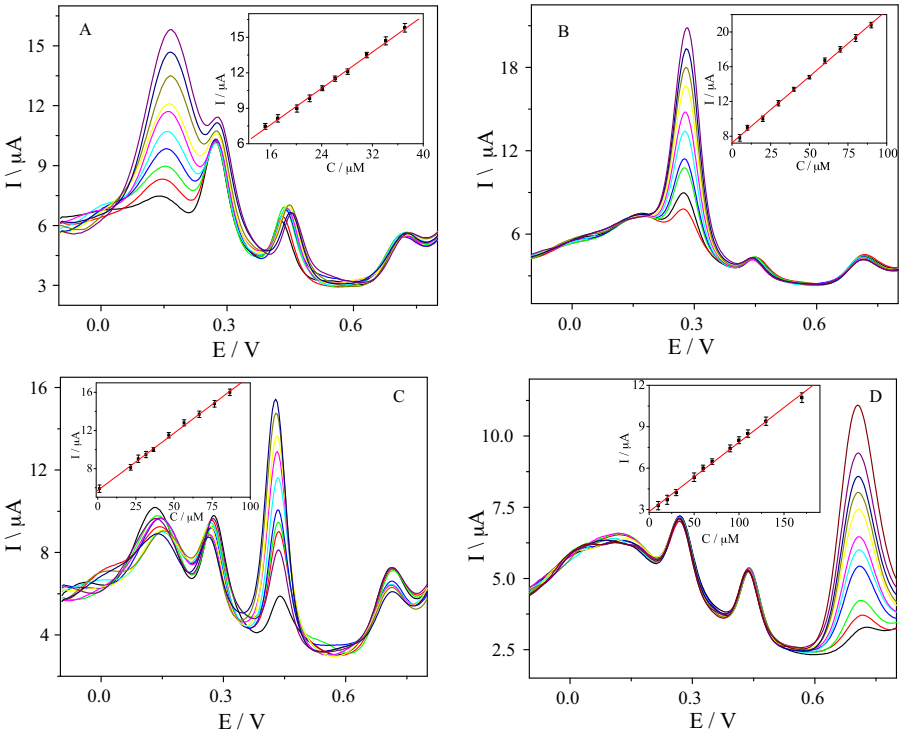

Fig. 3. DPVs at the nano-Au/*p*-TA/GCE in 0.1 M PBS (pH 4.0) (A) containing 20 μM UA, 10 μM DA, 40 μM NO_2^- and different concentrations of AA (from inner to outer): 15.1, 17.1, 20.1, 22.1, 24.1, 26.1, 28.1, 31.1, 34.1, 37.1 μM; (B) containing 160 μM AA, 20 μM UA, 40 μM NO_2^- and different concentrations of DA (from inner to outer): 5, 10, 20, 30, 40, 50, 60, 70 80, 90 μM; (C) containing 160 μM AA, 10 μM DA, 40 μM NO_2^- and different concentrations of UA (from inner to outer): 1.6, 11.6, 21.6, 26.6, 31.6, 36.6, 46.6, 56.6, 66.6, 76.6, 86.6 μM and (D) containing 160 μM AA, 20 μM UA, 10 μM DA and different concentrations of NO_2^- (from inner to outer): 10, 20, 30, 50, 60, 70 80, 90, 100, 110, 130, 170 μM. Insets: plots of I_p vs. concentration for AA, DA, UA and NO_2^-, respectively.

with a remarkable increase in peak current were observed at nano-Au/*p*-TA/GCE (curve d), which corresponded to AA, DA, UA and NO_2^-, respectively. The reasons may be ascribed as follows: first, metal nanoparticles, especially nano-Au usually causes very high electron transfer rate and enhances their currents towards the compounds; second, the *p*-TA film not only act as a promoter to accelerate the electrochemical reaction, but also lower the overpotential and separate the potentials of AA, DA and UA from each other (Sun and Wang, 2006). Third, the synergistic effect of the electrocatalytic activity of nano-Au and *p*-TA film resulted in the better catalytic property of nano-Au/*p*-TA/GCE towards AA, DA, UA and NO_2^- than that of other biosensors (Table 1S).

3.3. Simultaneous determination of AA, DA, UA and NO_2^-

The effect of pH value on the determination of AA, DA and UA in the mixture at nano-Au/*p*-TA/GCE was carefully investigated (Fig. 3S). In order to obtain high sensitivity and selectivity, pH 4.0 was selected for further experiments.

Differential pulse voltammetry (DPV) is employed to detect AA, DA, UA and NO_2^- due to its higher sensitivity and better resolution than CV. In fourfold mixture, the concentration of one species changed while the concentrations of the other three remained constant. The results were shown in Fig. 3A–D. Under optimal conditions, AA, DA, UA and NO_2^- could be determined in the ranges of 2.1–50.1 μM, 0.6–340.0 μM, 1.6–110.0 μM and 15.9–277.0 μM with the detection limits (S/N = 3) of 1.1×10^{-6} M, 5.0×10^{-8} M, 8.0×10^{-8} M and 8.9×10^{-7} M, respectively. The linear regression equations for AA, DA, UA and NO_2^- were expressed as $I_{p,AA}$ (μA) = 1.443 + 0.3855C_{AA} (μM) (R = 0.9976), $I_{p,DA}$ (μA) = 7.208 + 0.1528C_{DA} (μM) (R = 0.9983), $I_{p,UA}$ (μA) = 5.743 + 0.1196C_{UA} (μM) (R = 0.9976), I_{p,NO_2^-}(μA) = 2.850 + 0.05016$C_{NO_2^-}$(μm) (R = 0.9968), respectively. Inset showed calibration curve, respectively. The relative standard deviation (RSD) for determining AA, DA, UA and NO_2^- (n = 9) was 0.86%, 0.97%, 1.80% and 2.30%, respectively. These results were better than those of other obtained polymer film or metal nanoparticles modified electrodes (Wang et al., 2007; Yuan et al., 2008; Abdelwahab et al., 2009). The mechanisms behind the oxidation of AA, DA, UA and NO_2^- are concluded in the following. On the one hand, the *p*-TA film is permeable to both positively and negatively charged analytes. It is expected that anionic forms of AA, UA and NO_2^- were attracted by positively charged backbone of the *p*-TA film whereas positively charged DA was attracted by heteroatom of the *p*-TA film (Kalimuthu and John, 2009b, 2010). On the other hand, nano-Au not only separated the voltammetric signals of AA, DA, UA and NO_2^- but also enhanced their currents. Thus, enhanced peak currents were observed for AA, DA, UA and NO_2^- at nano-Au/*p*-TA modified electrode. Also, the DPVs obtained at the nano-Au/*p*-TA/GCE while the concentrations of AA, DA, UA and NO_2^- were simultaneously changed were investigated (Fig. 4S).

3.4. Interferences, stability and reproducibility

For investigating the anti-interference ability of the nano-Au/*p*-TA/GCE, several co-existing substances were selected. No significant interference for the detection of AA (200 μM), DA (10 μM), UA (20 μM) and NO_2^- (40 μM) was observed from the following compounds (μM): NaCl (5000), KCl (5000), $CaCl_2$ (5000), $MgSO_4$ (5000), $ZnCl_2$ (5000), glucose (1000), L-cysteine (300). The stability of the biosensor was also tested. After measurements, the modified electrode was stored at 4 °C. The peak current intensity only decreased 5.6%, 6.4%, 1.0% and 2.4% for AA, DA, UA and NO_2^- after 9 days, respectively. The relative standard deviation (RSD) (n = 8) for all these species was less than 2.3%. These results above indicate that the modified electrode shows a high selectivity, well stability and good reproducibility.

3.5. Sample analysis

Human urine and serum samples were selected as real samples for analysis using the standard adding method. All samples were diluted with 0.1 M PBS (pH 4.0). In order to ascertain the correctness of the results, the diluted samples mentioned above were spiked with certain amounts of AA, DA, UA and NO_2^- and then were detected. The results are presented in Tables 2S and 3S. The recovery rates of the samples ranged between 91.0% and 109.0%, indicating the proposed method could be effectively used for the determination of AA, DA, UA and NO_2^- in real samples.

4. Conclusions

In conclusion, a novel biosensor has been fabricated based on the construction of *p*-TA film further modified with nano-Au. Moreover, the biosensor not only exhibited high electrocatalytic activities towards the oxidation of AA, DA, UA and NO_2^-, but also resolved the overlapping peaks, lowered the overpotential, and greatly enhanced the current response. Furthermore, compared with nano-Au/GCE and *p*-TA/GCE, the nano-Au/*p*-TA/GCE modified with both *p*-TA and nano-Au could facilitate the simultaneous determination of AA, DA, UA and NO_2^- with high sensitivity and selectivity. The future work will be focused on using the biosensor for the simultaneous determination of AA, DA, UA and NO_2^- in clinical test.

Acknowledgments

The National Natural Science Foundation of China (21075100), the Ministry of Education of China (Project 708073), the Nature Science Foundation of Chongqing City (CSTC-2009BA1003, 2011BA7003) specialized research fund for the Doctoral Program of Higher Education (20100182110015) and State Key Laboratory of Electroanalytical Chemistry (SKIEAC 2010009), China supported this work.

Appendix A. Supplementary data

Supplementary data associated with this article can be found, in the online version, at doi:10.1016/j.bios.2011.08.035.

References

Atta, N.F., El-Kady, M.F., Galal, A., 2010. Anal. Biochem. 400, 78–88.
Abdelwahab, A.A., Lee, H.M., Shim, Y.B., 2009. Anal. Chim. Acta 650, 247–253.
Baraldi, M., Malavasi, W., Grandi, R., 1996. J. Chem. Crystallogr. 26, 63–66.
Deng, C.Y., Chen, J.H., Wang, M.D., Xiao, C.H., Nie, Z., Yao, S.Z., 2009. Biosens. Bioelectron. 24, 2091–2094.
Ensafi, A.A., Khayamian, M.T.T., 2009. J. Electroanal. Chem. 633, 212–220.
Gopalan, A.I., Lee, K.P., Manesh, K.M., Santhosh, P., 2007. Talanta 71, 1774–1781.
Guevara-Guzmam, R., Emson, P.C., Kendrick, K.M.J., 1994. J. Neurochem. 62, 807–810.
Huang, J.S., Liu, Y., Hou, H.Q., You, T.Y., 2008. Biosens. Bioelectron. 24, 632–637.
Harish, S., Mathiyarasu, J., Phani, K.L.N., Yegnaraman, V., 2008. J. Appl. Electrochem. 38, 1583–1588.
Kalimuthu, P., John, S.A., 2010. Talanta 80, 1686–1691.
Kalimuthu, P., John, S.A., 2009a. Bioelectrochemistry 77, 13–18.
Kalimuthu, P., John, S.A., 2009b. Anal. Chim. Acta 647, 97–103.
Liu, X.G., Peng, Y.H., Qu, X.J., Ai, S.Y., Han, R.X., Zhu, X.B., 2011. J. Electroanal. Chem. 654, 72–78.
Lin, X.H., Zhang, Y.F., Chen, W., Wu, P., 2007a. Sens. Actuators B 122, 309–314.
Lin, X.H., Zhuang, Q., Chen, J.H., Zhang, S.B., Zheng, Y.J., 2007b. Sens. Actuators B 125, 240–245.
Li, Y.X., Lin, X.Q., 2006. Sens. Actuators B 115, 134–139.
Sun, Y.X., Wang, S.F., Zhang, X.H., Huang, Y.F., 2006. Sens. Actuators B 113, 156–161.
Sun, Y.X., Wang, S.F., 2006. Microchim. Acta 154, 115–121.
Thiagarajan, S., Chen, S.M., 2007. Talanta 74, 212–222.
Wang, P., Li, Y.X., Huang, X., Wang, L., 2007. Talanta 73, 431–437.
Yuan, Y., Ahammad, A.J.S., Xu, G.R., Kim, S., Lee, J.J., 2008. Bull. Korean Chem. Soc. 29, 1883–1884.
Zhang, Y., Yuan, R., Chai, Y.Q., Li, W.J., Zhong, X., Zhong, H.A., 2011. Biosens. Bioelectron. 26, 3977–3980.
Zhu, S.Y., Li, H.J., Niu, W.X., Xu, G.B., 2009. Biosens. Bioelectron. 25, 940–943.
Zhang, R., Jin, G.D., Chen, D., Hu, X.Y., 2009. Sens. Actuators B 138, 174–181.